SIMPLIFIED FINITE ELEMENT MODELLING OF ACOUSTICALLY TREATED STRUCTURES

M. CARFAGNI, P. CITTI AND M. PIERINI

Dipartimento di Meccanica e Tecnologie Industriali, Università di Firenze,
Via di Santa Marta 3, 50139 Firenze, Italy

The application of non-optimized damping and phono-absorbent materials to automotive systems has not proved fully satisfactory in abating noise and vibration. The objective of this work was to develop a simple finite element modelling procedure that would allow optimizing structures such as a car body-in-white in terms of vibroacoustic behavior from the design stage. A procedure was developed to determine the modifications to be made in the mass, stiffness and damping characteristics in the finite element (FE) modelling of a metal structure meshed with shell elements so that the model would describe the behavior of the acoustically treated structure. To validate the modifications, a numerical–experimental comparison of the velocities on the vibrating surface was carried out, followed by a numerical–experimental comparison of the sound pressures generated by the vibrating plate. In the comparison a simple monopole model was used, in which each area of vibrating surface could be likened to a point source. The simulation and experimental procedures, previously validated for the metal structure, were then applied to multi-layered panels. Good agreement between the experimental and simulated velocities and sound pressures resulted for all the multi-layered panel configurations examined.

© 1997 Academic Press Limited

1. INTRODUCTION

The abatement of noise and vibrations has always been a major goal in vehicle design. Over the last few years, as a result of the growing strictness of international standards and the criticality of user comfort in the success or failure of new models, its importance has increased even more.

The rewards for abating noise and vibration are well worth the effort. In addition to enhanced user comfort, benefits are also accrued to the vehicle itself in terms of performance and longer lifetimes for its electrical, electronic and mechanical components. However, the conventional approach to noise and vibration abatement, which mainly involves the application of panels made of damping and phono-absorbent materials that have not been subjected to prior optimization, can no longer be considered satisfactory.

Of notable aid would be the availability of a tool to optimize a structure, such as a car body-in-white, in terms of its vibroacoustic behavior right from the initial design stage. Obviously, the ability to design a car body in relation to noise would represent a breakthrough in current vehicle design, since the car body is the main source of vibration transmission from the mechanical components and the road surface to the passengers.

The objective of this work, the theoretical background and preliminary phase of which have been described in a previous paper [1], was to determine how to modify the mass, stiffness and damping characteristics in the finite element (FE) modelling of a metal structure meshed with shell elements to enable the model to describe the behavior of the acoustically treated structure (normally a multi-layered panel). To validate the

modifications, a numerical–experimental comparison of the velocities on the vibrating surface was carried out, followed by a numerical–experimental comparison of the ensuing sound pressures. For the second phase, a simple monopole model, in which each area of vibrating surface could be likened to a point source, was developed to evaluate the sound pressure generated by the vibrating surface. In this work, the simulation and experimental procedures validated for the metal structure in the previous work, have been applied to multi-layered panels.

2. THEORETICAL BACKGROUND

When a structure is excited by a force, $F = F(t)$, varying in time, and is made to vibrate, it displaces the air particles adjacent to its surface, which in turn vibrate around their equilibrium position, thus displacing the other particles that they are in contact with. This mechanism transforms the structure's vibrational mechanical energy into acoustic energy in the form of an acoustic wave that propagates into the surrounding environment. Knowing the system's excitation, one can calculate the sound pressure in the environment by means of a transfer function that characterizes the vibrations' structural path and the radiated sound pressure field. Hence, assuming system linearity, one can relate the value of the sound pressure $P = P(x, y, z, t)$ at a point i in space to the excitation force applied at point j by a frequency response function (FRF) of the kind

$$H_{FP} = P/F. \tag{1}$$

(A list of nomenclature is given in the Appendix.)

Consider the vibrating structure as a plate divided into rectangles, each of which is considered a monopole. Each source's contributions can be viewed as the product of two FRFs, in which the first relates each vibrating component's velocity to the exciting force on point i and the second relates the sound pressure field at point j in space to the vibrating component's velocity. Hence, assuming

$$H_{FV} = V_k/F_i \qquad \text{and} \qquad H_{VP} = P_j/V_k, \tag{2}$$

one obtains

$$H_{FP} = \sum_{k=1}^{n} H_{FV} H_{VP}, \tag{3}$$

where n represents the number of areas into which the structure is divided.

Analyzing the two terms inside the summation, one can see that the first, H_{FV}, can be experimentally determined by direct measurement or analytically determined by modelling the structure with finite elements. To simulate the second term, H_{VP}, influenced by the environment in which the sound propagates, the authors have developed a simple monopole model, assuming that each rectangular element of the modelled plate emits a spherical wave. Hence, one can express H_{VP} [1–3] as

$$H_{VP} = \frac{P_j}{V_k} = \frac{P(r, t)}{u(r, t)} = -\frac{\mathrm{j}\omega\rho r_0^2}{\left(\mathrm{j}\dfrac{\omega}{c} r_0 - 1\right) r} \, \mathrm{e}^{\mathrm{j}(\omega/c)(r - r_0)}. \tag{4}$$

3. PROCEDURE

3.1. VERIFICATION OF THE MODELLING TECHNIQUE

A procedure was developed to verify whether the modified FE modelling of the vibrating plates produced good agreement with the actual experimental results in terms of vibration and noise generation. The procedure entailed a step-by-step numerical–experimental comparison of the H_{FP} applied to flat steel plates (measuring $550 \times 350 \times 1$ mm) without acoustic treatment [1]. In the first phase of the verification, the experimentally measured H_{FV} and the H_{VP} calculated with the monopole model were used: the monopole model could thus be adjusted by comparing the experimental and numerical values of the H_{FP}. The H_{FV} were then computed with the FE model and combined with the calculated H_{VP}. The resulting H_{FP} was compared to the experimental one. The excellent results of the comparison (see Figure 1) justified development of the entire procedure. The procedure, which is described in this work, was applied to multi-layered panels of the same configuration as those actually used in automotive applications, first with a damping material glued to the steel plate, and then with the addition of a porous material and a high mass viscoelastic material (septum) resting upon the other layers without any adhesive.

The test rig is schematically illustrated in Figure 2. The test plate was fixed along its external perimeter to a rigid frame within the frequency range being examined. The plate was supported by four springs, which provided motion to the rigid frame at frequencies below the test range. An electromagnetic shaker was used to produce vibration, while an impedance head between the shaker and frame allowed measurement of the applied force.

The velocities were obtained by integrating the accelerations measured on the plate by a lightweight accelerometer in order to prevent the mass from affecting dynamic behavior. Sound pressure was measured at various positions above the plate by microphones placed at various locations above the test rig, which was housed inside a semi-anechoic chamber. The rig was encapsulated in an acoustically treated isolation box to ensure that the microphones measured only the noise generated by the plate's upper surface.
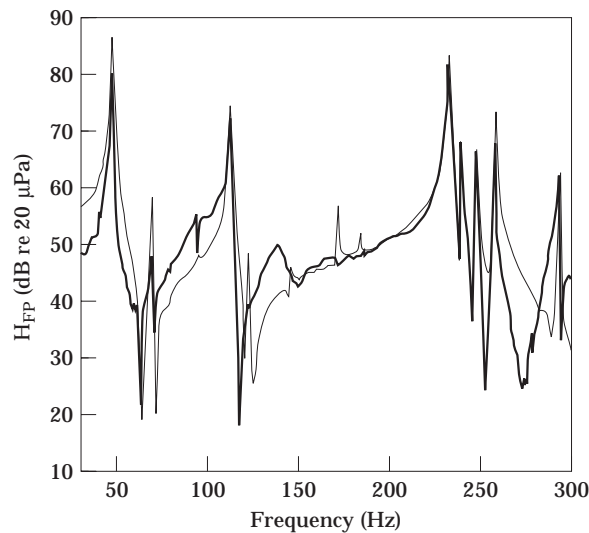

Figure 1. A plate without acoustic treatment. ——, Measured H_{FP} values; ——, H_{FP} values simulated on the basis of simulated H_{VP}.
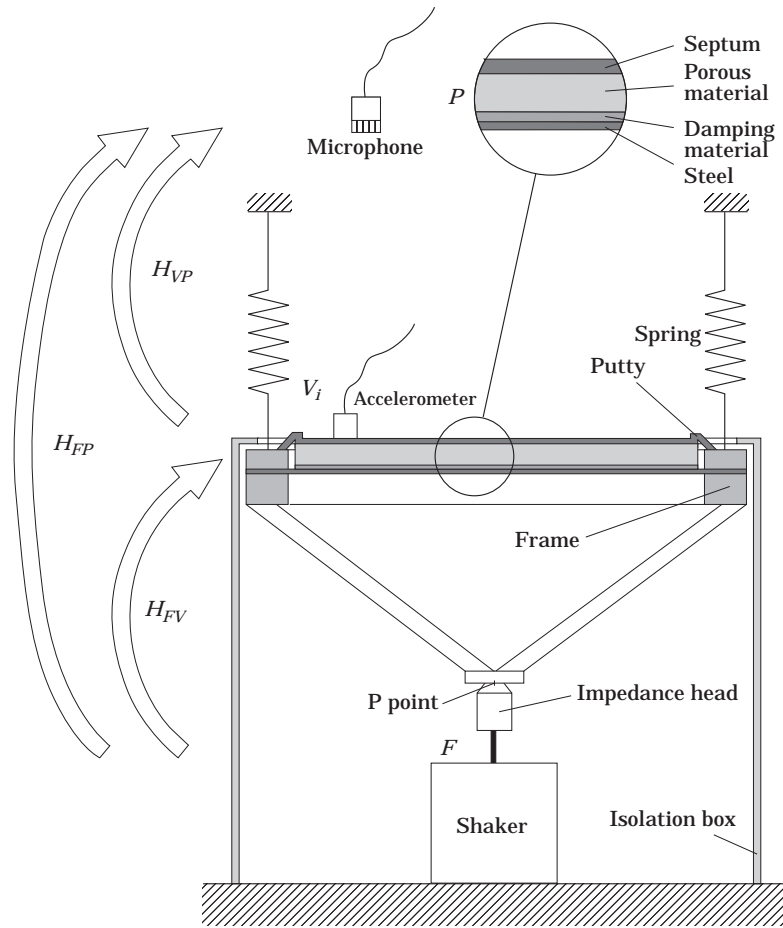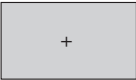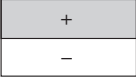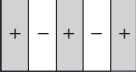
Figure 2. A schematic of the test rig.

3.2. PROBLEMS IN THE EXCITATION SYSTEM

In the experimental modal analysis of the plate, an odd phenomenon emerged from comparison of the experimental and FE results. More natural frequencies were encountered in the same frequency range in the FE simulation than in experimental testing. Two (specifically numbers 5 and 9 in Table 1) had seemingly vanished altogether. Examination of the displacement at point P (see Figure 2) for each mode vibration in the FE model reveals amplitudes between seven and eight orders of magnitude smaller than those of the other eigenvectors (scaled to unitary modal mass) at the vanished natural frequencies. This means that if a modal synthesis between point P and the plate points starting from the FE eigenvectors is performed, one obtains the FRFs in which modes 5 and 9 are invisible, owing to the negligible amplitudes of their eigenvectors. The result is thus synthesized FRFs closely resembling the experimentally derived ones. To explain this behavior, it should be recalled that the plate had dual symmetry with respect to the centerpoint axes and was clamped on all four sides. One can now discover the source of this oddity. Calling R the resultant of the inertial forces acting on the plate and M their resultant moment, one can first analyze the mode shapes for the various natural frequencies. The following three cases are shown in Table 1: (1) the mode shapes are symmetric to both axes of symmetry, so that $R \neq 0$ and $M = 0$; (2) the mode shapes

TABLE 1

The characteristics of the first ten modes for inertial forces (R), their resultant moments (M) and types of symmetry

Mode	Shape	R	M	Types of symmetry
1	`[ + ]`	$\neq 0$	0	Symmetric Symmetric
2	`[+	−]`	0	$\neq 0$	Symmetric Asymmetric
3	`[−	+	−]`	$\neq 0$	0	Symmetric Symmetric
4	`[ + ] / [ − ]`	0	$\neq 0$	Asymmetric Symmetric
5	`[+	−] / [−	+]`	0	0	Asymmetric Asymmetric
6	`[+	−	+	−]`	0	$\neq 0$	Symmetric Asymmetric
7	`[+	−	+] / [−	+	−]`	0	$\neq 0$	Asymmetric Symmetric
8	`[ − ] / [ + ] / [ − ]`	$\neq 0$	0	Symmetric Symmetric
9	`[+	−	+	−] / [−	+	−	+]`	0	0	Asymmetric Asymmetric
10	`[+	−	+	−	+]`	$\neq 0$	0	Symmetric Symmetric

are symmetric to one axis of symmetry and asymmetric to the other, so that $R = 0$ and $M \neq 0$; (3) the mode shapes are asymmetric to both axes of symmetry, so that $R = 0$ and $M = 0$. Classifying the plate's natural frequencies, one can observe that "vanishing" modes 5 and 9 are the only ones belonging to case 3.

Mode 5, schematically illustrated in Figure 3, will serve as an example. Since $R = 0$ and $M = 0$ according to the theorem of centerpoint motion, the center point G is immobile and consequently all the points belonging to the nodal lines of AC and BD in Figure 3 are immobile, and the frame supporting and constraining the plate is also immobile. Hence, the whole frame, and also the application point of force F during the experimental FRF measurement, fails to move during the vibration of the plate at that given natural frequency. This, on the one hand, justifies the exceedingly reduced amplitude of the displacements of point P encountered in modes 5 and 9 in the FE solution and, on the other, explains why they failed to emerge experimentally. The frame, which was excited
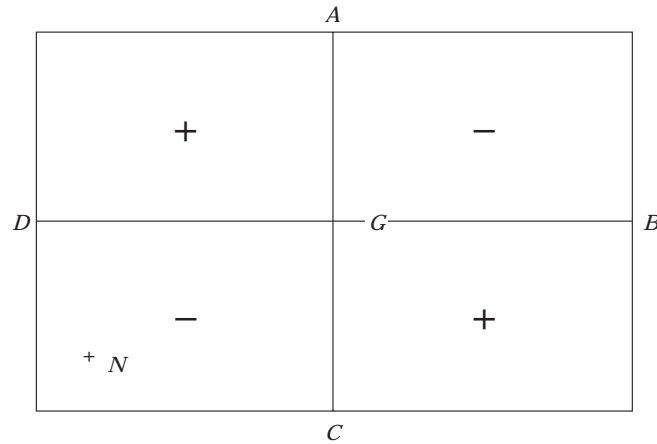
Figure 3. A representation of the mode shape of mode 5.

at point P in order to make the plate vibrate, was thus excited in one of its modal nodes and one was thus unable to transmit energy to the plate at that particular frequency.

To resolve the problem caused by the mass distribution, it was necessary to insert a 20 g "unbalancing" mass on the plate. The mass was placed at point N, which is characterized by not belonging to any nodal lines for the modes under examination. In this way, all the modes emerged in both the experimental and numerical analyses.

4. RESULTS

4.1. RESULTS FOR THE STEEL PLATE WITH DAMPING MATERIAL

The steel plate was tested with layers of damping material of various thicknesses. Although all gave good results, for brevity only one is illustrated. The thickness of the damping material was 1·86 mm and the surface density was 3·37 kg/m². The material was hot-glued to the steel plate in an oven for 30 minutes at 160°C, according to the manufacturer's instructions. As had been previously done for the untreated plates [1], the plate was divided into 96 rectangles, each measuring 45·8 × 43·8 mm. The velocities measured at their centerpoints were respectively associated to each rectangle.

Following the previously described procedure, the 96 H_{FV} were measured and together with the numerically derived H_{VP} from the monopole model, produced the H_{FP} plotted in Figure 4 against the experimentally measured value. The good agreement between the two curves allowed passing to the next step, the FE modelling of the plate.

The first step was to analyze the plate experimentally to derive its natural frequency, damping and mode shapes. At the same time, an FE model was created by using shell elements for the plate and beam elements for the frame beams. The modifications to the FE model of the untreated plate entailed replacing the density by an equivalent density to account for the mass owing to the damping material and replacing the thickness by an equivalent thickness to account for the increased stiffness resulting from the treatment. While the calculation for the density modifications was fairly straightforward, the thickness variation had to be evaluated by trial and error in order to provide a good fit for the numerical and experimental natural frequencies.

The equivalent density was 10 333 kg/m³ (+32 percent); the equivalent thickness, 1·06 mm (+6 percent). Since the objective of this work was to characterize the variations to be made to the FE model of a shell structure in terms of mass, stiffness and damping
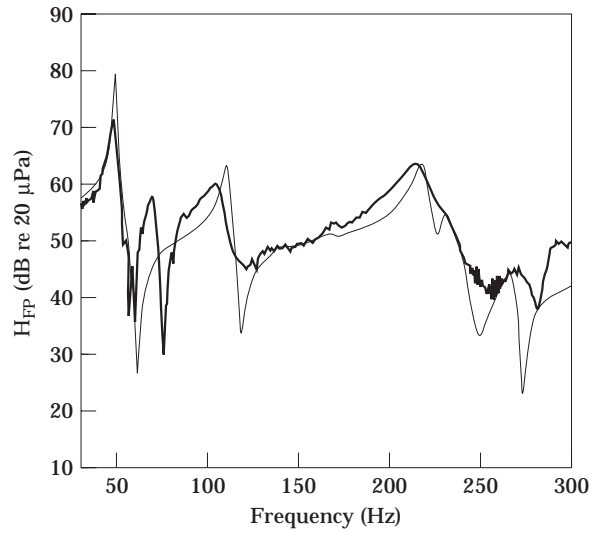
Figure 4. A plate with damping material. ——, Measured H_{FP} values; ——, H_{FP} simulated on the basis of measured H_{FV}.

in order to simulate vibroacoustic treatment, the calculation of an equivalent thickness could represent a serious limitation. It should, however, be noted that the variation was so slight that neglecting it did not produce any significant errors. In addition, when simulating a structure stiffer than a flat plate (e.g., a grooved surface), one can expect the stiffness contribution of the damping material to be negligible and hence can refer to the thickness of a plate lacking acoustic treatment.

With the frequency and the mode shapes calculated by using the FE model and the dampings derived from experimental measurements by using LMS software, it was possible to synthesize the H_{FV}. The synthesized and experimental H_{FV} relative to one of the measuring points are plotted in Figure 5. The synthesized H_{FV} associated to H_{VP} derived
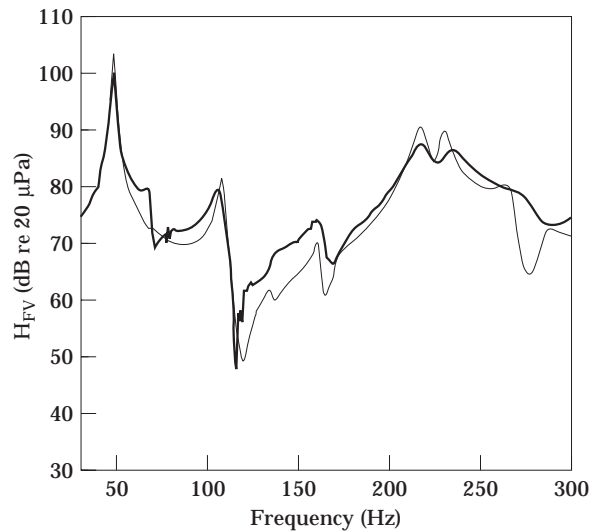

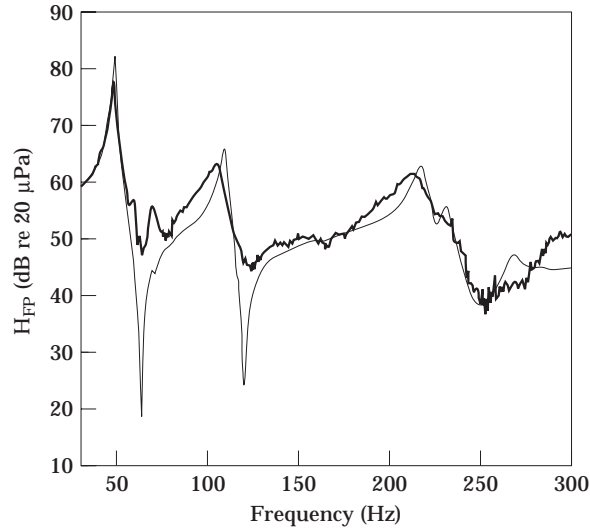Figure 5. Measured (——) and simulated (——) H_{FV} values for a point of a plate with damping material.

Figure 6. A plate with damping material: —— , Measured H_{FP} values; ——, H_{FP} values simulated on the basis of simulated H_{FV}.

from the monopole model produce the H_{FP} in Figure 6, which were compared with the experimental FRFs. The good agreement between the two curves justified proceeding to the addition of layers in modelling the multi-layered panel. Good agreement also emerged when the sound pressure measuring point was varied.

4.2. TEST RESULTS FOR THE STEEL PLATE WITH DAMPING MATERIAL, POROUS LAYER AND SEPTUM

A steel plate in various configurations of damping material + porous layer + septum was tested. For brevity, only the results for a configuration comprising a 10 mm thick
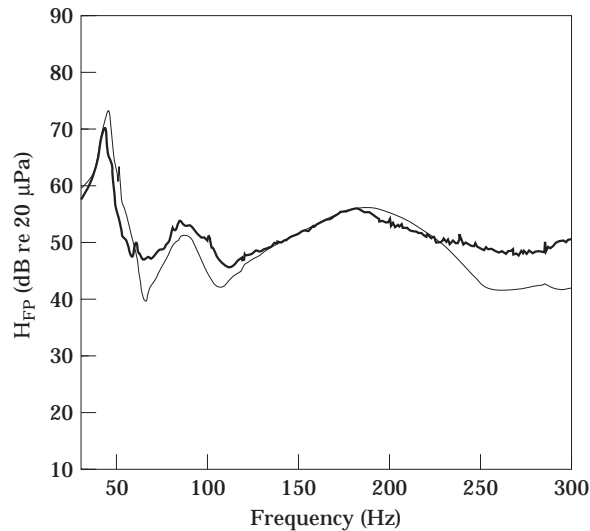

Figure 7. A plate with damping material, porous layer and septum: —— , Measured H_{FP} values; ——, H_{FP} values simulated on the basis of H_{FV} values measured on the upper panel plate surface.

porous layer and a septum layer with a surface density of 5 kg/m^2 are illustrated. The two layers were glued together according to the manufacturer's specifications and the resulting layer was placed over the test plate. Putty was applied along the edge of the multi-layered
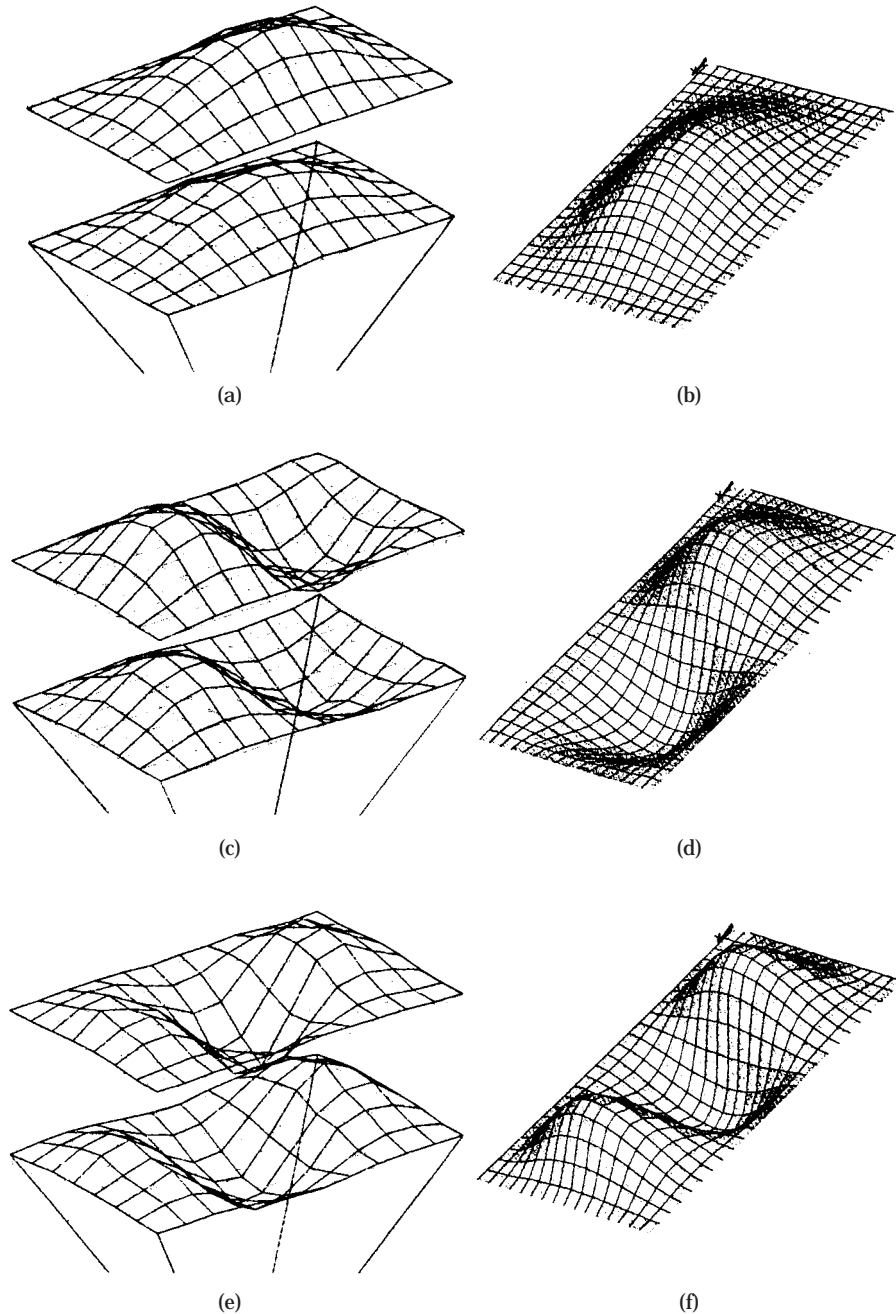

(a)

(b)

(c)

(d)

(e)

(f)

Figure 8. The first numerical and experimental frequencies and mode shapes of the steel plate with damping material, porous layer and septum. (a) Experimental mode 1; $f = 42$ Hz, damping = 3 percent: (b) numerical mode 1; $f = 41$ Hz: (c) experimental mode 2; $f = 60$ Hz, damping = 5 percent: (d) numerical mode 2; $f = 59$ Hz: (e) experimental mode 3; $f = 86$ Hz, damping = 12 percent: (f) numerical mode 3; $f = 93$ Hz.
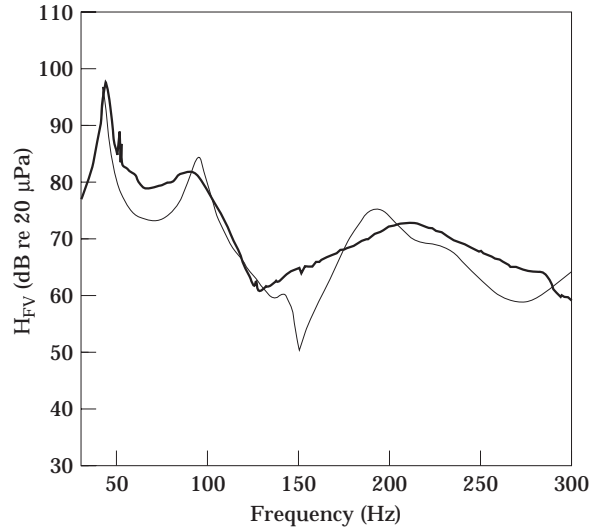
Figure 9. Measured (———) and simulated (———) H_{FV} values for a point of a plate with damping material, porous layer and septum.

panel (see Figure 2) to connect the panel to the frame edges. This was done to prevent an acoustic flow through the edges and to stimulate real-life automotive applications, in which the multi-layered panels are connected to the car bodies by the upholstery. As in the preceding case, in Figure 7 is shown the H_{FP} estimated on the basis of the experimental H_{FV} measured on the upper panel surface plotted in comparison with the experimental H_{FP} curve.

   The mode shapes on the upper and lower surfaces were measured by experimental modal analysis. The first three mode shapes are shown in Figure 8. There is excellent agreement, especially for the low frequencies, which are those of interest in automotive applications,
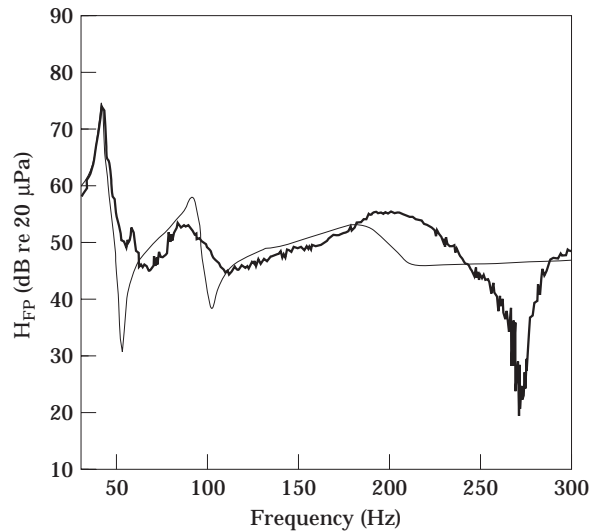

Figure 10. A plate with damping material, porous layer and septum: ———, Measured H_{FP} values; ———, H_{FP} values simulated on the basis of H_{FV} values simulated.

between the upper and lower surface mode shapes. This is an extremely important result in view of the FE modelling of the multi-layer panel with only a single shell layer. In this case, the modifications to the FE model of the untreated plate are analogous to those of the previous cases: an equivalent density of 13 956 kg/m³ ($+77\cdot8$ percent); an equivalent thickness of $1\cdot13$ mm ($+13$ percent). The same considerations as in the previous case are also applicable here.

The frequencies and mode shapes obtained from the FE model are shown in Figure 8 in comparison with the experimental mode shapes. The numerical–experimental comparison of the H_{FP} calculated on the basis of the synthesized H_{FV} plotted with the experimental H_{FP} curve in Figure 9 is illustrated in Figure 10. The good agreement validates the procedure for evaluating the modifications for the plate FE model with acoustic treatment and the validity of the modifications selected for simulating the treatment of the experimental multi-layered panels.

Owing to the high levels, not all damping modes could be experimentally determined with the LMS software; some had to be obtained by interpolation. Since damping and mass emerged as the parameters having the strongest effect on dynamic behaviour, a forthcoming research project will be aimed at devising a reliable experimental procedure for evaluating damping (mass being far easier to compute).

5. CONCLUSIONS

A simplified procedure for the finite element modelling of acoustically treated structures such as a car body-in-white has been presented. The vibroacoustic behavior of multi-layered panels was simulated by varying mass (density), stiffness (thickness) and damping in steel plate. Good agreement between the experimental and simulated velocities and sound pressures resulted for all the multi-layered panel configurations examined. The procedure is simple to use, requires little calculation effort, and may be applied to FE models of vibrating panels only by varying their mass and stiffness. Since damping must be experimentally determined for each panel configuration, our next work will focus on developing a procedure for evaluating damping, the complexity of which increases as the damping level increases.

REFERENCES

1. M. CARFAGNI, P. CITTI and M. PIERINI 1994 *Basic Metrology and Applications*. Turin, Italy: Levrotto & Bella. See pp. 135–140. A method for evaluating the sound pressure field generated by a vibrating system.
2. D. J. EWINS 1986 *Modal Testing*: *Theory and Practice*. Letchworth, Hertfordshire, U.K.: Research Studies Press. See pp. 48–52.
3. P. M. MORSE and K. U. INGARD 1968 *Theoretical Acoustics*. Princeton, New Jersey: Princeton University Press. See pp. 309–311.
4. L. L. BERANEK and I. L. VER 1992 *Noise and Vibration Controls Engineering*: *Principles and Applications*. New York: John Wiley. See pp. 272–279.

APPENDIX: NOMENCLATURE

c	sound speed
$F(t)$	force in relation to time
H_{FP}	force–sound pressure frequency response function
H_{FV}	force–velocity frequency response function
H_{VP}	velocity–sound pressure frequency response function
j	imaginary unit ($\mathrm{j}^2 = -1$)
$P(r, t)$	sound pressure in relation to the distance from the spheres (polar co-ordinates)
r	distance of a point from the center of the sphere
r_0	sphere radius
$u(r, t)$	velocity of the air particles in relation to the distance from the sphere and time
V_k	velocity of the k vibrating component
ρ	air density
ω	$2\pi f$, circular frequency